

Coexistence of localized and itinerant carriers near T_C in calcium-doped manganites

M. Jaime*, P. Lin, S. H. Chun, M. B. Salamon P. Dorsey[§] and M. Rubinstein[§]

Department of Physics and Materials Research Laboratory

University of Illinois at Urbana-Champaign

1110 W. Green Street, Urbana, IL 61801

§ U.S. Naval Research Laboratory, Washington D.C. 20375-5000

(April 12, 2018. revised version)

Abstract

We explore the possibility that polaronic distortions in the paramagnetic phase of $\text{La}_{0.67}\text{Ca}_{0.33}\text{MnO}_3$ manganites persist in the ferromagnetic phase by considering the observed electrical resistivity to arise from coexisting field- and temperature-dependent polaronic and band-electron fractions. We use an effective medium approach to compute the total resistivity of the two-component system, and find that a limit with low percolation threshold explains the data rather well. To test the validity of this model, we apply it to the thermoelectric coefficient. We propose a plausible mean-field model that reproduces the essential features of a microscopic model and provides a comparison with the experimental mixing fraction, as well as the magnetization and magnetic susceptibility.

75.10.-b, 75.70.Pa, 72.20.-i, 72.20.Pa, 75.30.Cr

Typeset using REVTeX

*Present address Los Alamos National Laboratory, MSK764, Los Alamos, NM 87545

There is a growing consensus that the so-called colossal magnetoresistivity (CMR) of $\text{La}_{1-x}\text{A}_x\text{MnO}_3$, where A is a divalent substituent, is larger when both *double exchange* and *strong coupling to local lattice deformations* are involved. [1–4] In the double exchange model, [5,6] electrons can hop from the singly occupied e_{2g} orbital of Mn^{3+} ions to empty e_{2g} orbitals of neighboring Mn^{4+} ions. Strong Hund’s-rule coupling enhances the hopping matrix element when the $S = 3/2$ t_{2g} cores of the neighboring sites are aligned, thereby favoring ferromagnetism and an increased bandwidth. However, as Millis and coworkers [1,7] have emphasized, the Jahn-Teller effect in Mn^{3+} , if strong enough, can lead to polaron formation and the possibility of self-trapping. The effective Jahn-Teller coupling constant λ_{eff} , in this picture, must be determined self-consistently, both because it depends inversely on the bandwidth and because the effective transition temperature increases with decreasing λ_{eff} . If λ_{eff} is larger than a critical value λ_c , the system consists of polarons in the paramagnetic phase. As the temperature is lowered to the Curie temperature T_C , the onset of ferromagnetism increases the effective bandwidth, which reduces λ_{eff} , thereby increasing the effective transition temperature. As a result, the polarons may dissolve into band electrons if λ_{eff} drops below λ_c and the material reverts to a half-metallic, double exchange ferromagnet at low temperatures.

In the Millis *et al.* model, the tendency toward polaron formation is monitored by a local *displacement* coordinate r , which is zero for $\lambda_{eff} < \lambda_c$, and grows continuously as λ_{eff} increases beyond that value. However, polarons are typically [8] bimodal—large or small—so that we should consider r to be a measure of the relative proportion of large polarons (band electrons for which $r \approx 0$) and small polarons (for which r is an atomic scale length). Indeed, there is growing experimental evidence [9–12] that polaronic distortions, evident in the paramagnetic state, persist over some temperature range in the ferromagnetic phase. This paper explores that possibility, in the effective medium approximation, by considering the observed electrical resistivity to arise from a field- and temperature-dependent concentration $c(H, T)$ of metallic regions within a semiconductive, polaronic background having an activated electrical conductivity. [13] We test the validity of this model by applying it to the thermoelectric coefficient, also within the effective medium approximation, and extract $c(H, T)$ for stripe-like domains. We propose a mean-field model, in which $c(H, T)$ is a secondary order parameter, that reproduces the qualitative features of the experimental data.

The $\text{La}_{2/3}\text{Ca}_{1/3}\text{MnO}_3$ film samples used in this study were prepared by pulsed laser deposition onto LaAlO_3 substrates to a thickness of $0.6 \mu\text{m}$. As described previously [14], they were annealed at $1000 \text{ }^\circ\text{C}$ for 48 hr. in flowing oxygen. Measurements were carried out in a 7 T Quantum Design Magnetic Property Measurement System with and without an oven option provided by the manufacturer. A modified sample rod brought electrical leads and type-E thermocouples to the sample stage. A bifilar coil of $12 \mu\text{m}$ Pt wire was calibrated to serve both as a thermometer and to provide a small heat input for the thermopower measurements. Measurements in fields up to 7 T could be carried out over the temperature range $4 \text{ K} \leq T \leq 500 \text{ K}$. Following the transport measurements, magnetization data $M(H, T)$ were acquired up to 380 K by conventional methods.

Figure 1 shows the magnetization and resistivity data over the temperature range of interest. The data below 200 K exhibit essentially field independent, metallic behavior, and are well fit by a power law,

$$\rho_{lt}(T) = [0.22 + 2 \times 10^{-5} \text{ K}^{-2}T^2 + 1.2 \times 10^{-12} \text{ K}^{-5}T^5] \text{ m}\Omega \text{ cm}. \quad (1)$$

Above 260 K, the resistivity is exponential and again independent of field, given [15] by the form expected for the adiabatic hopping of small polarons,

$$\rho_{ht}(T) = (1.4\mu\Omega \text{ cm K}^{-1})T \exp(1276 \text{ K}/T). \quad (2)$$

Both limits are displayed in Figure 1 as dotted lines. Our assumption is that these represent the resistivity of band electrons and polarons, respectively, and that the transition region can be represented by the conductivity of an effective medium [13] characterized by a mixing factor $c(H, T)$ which we envisage to be the fraction of the carriers that are in the metallic state. We assume the effective resistivity $\rho(H, T)$ to satisfy the general expression for ellipsoidal metallic regions (resistivity $\rho_{lt}(T)$) embedded in a semiconducting matrix (resistivity $\rho_{ht}(T)$) [16],

$$\frac{c(\rho - \rho_{lt})}{3} \left[\frac{1}{\rho_{lt} + g_{\parallel}(\rho - \rho_{lt})} + \frac{2}{\rho_{lt} + g_{\perp}(\rho - \rho_{lt})} \right] + \frac{3(1-c)(\rho - \rho_{ht})}{2\rho_{ht} + \rho} = 0. \quad (3)$$

Here, $g_{\perp} \simeq 1/2$, $g_{\parallel} = (b^2\rho_{ht}/a^2\rho) \ln[1 + (a\rho/b\rho_{ht})]$ and a, b are the (major, minor) axes of the prolate ellipsoids. As a first approximation, we set $c(0, T) = M(0, T)/M_{sat}$, using the data of Fig. 1a. The chain curves in Fig. 1b show that the magnetization roughly reproduces the shape of the resistivity curves at zero field. That the metallic resistivity switches on quickly as the system orders indicates a low percolation threshold and a large aspect ratio ($a \gg b$). This suggests that the metallic regions appear as stripe domains, rather than as compact clusters. The magnetization does not approximate, at all, the relative concentrations in applied fields, as seen in the solid line in Fig. 1b. As an alternative, we solve Eq. (3) for $c(H, T)$ using the experimental resistivity $\rho_{exp}(H, T)$, with the result shown in Fig. 2a for $a/b = 50$.

As a second test of this approach, we consider the Seebeck coefficient $S(H, T)$, measured over the same temperature range, and plotted in Fig. 2b. We fit the low temperature thermopower arbitrarily to a power law

$$S_{lt}(T) = [(0.051 \text{ K}^{-1})T - (1.3 \times 10^{-4} \text{ K}^{-2})T^2 - (3.2 \times 10^{-7} \text{ K}^{-3})T^3] \mu\text{V}/\text{K}, \quad (4)$$

and the high temperature data [15] to the form expected for small polarons,

$$S_{ht}(T) = [(9730 \text{ K})T^{-1} - 29] \mu\text{V}/\text{K}. \quad (5)$$

Low and high temperature limits are displayed as dotted lines in Figure 2b. A remarkable feature of the transport properties of composites is that knowing any two effective transport properties and those of the constituents determines the third. [17] A closed expression for the Seebeck coefficient has been derived by Bergman and Stroud [18] which, by recognizing that the effective conductivities match the high and low temperature values in the respective limits, we can write in the following form,

$$S(H, T) = \frac{(S_{lt} - S_{ht})(\kappa_{lt} - \kappa_{ht})}{(\kappa_{ht}\rho_{ht} - \kappa_{lt}\rho_{lt})} \frac{\rho_{lt}\rho_{ht}}{(\rho_{ht} - \rho_{lt})} + \frac{(S_{lt}\rho_{ht} - S_{ht}\rho_{lt})}{(\rho_{ht} - \rho_{lt})} + \frac{(S_{ht} - S_{lt})\kappa(H, T)\rho(H, T)}{(\kappa_{ht}\rho_{ht} - \kappa_{lt}\rho_{lt})}. \quad (6)$$

Here, κ_{lt} , κ_{ht} , and $\kappa(H, T)$ are the thermal conductivities of low and high temperature phases and the effective medium, respectively. While small changes in $\kappa(H, T)$, of order 20% in the transition region, have been reported [19], the thermal conductivity of this thin-film sample is dominated by the substrate. All three thermal conductivities are, therefore, equal at each temperature-field point, enabling us to simplify the expression to,

$$S(H, T) = \frac{1}{\rho_{ht} - \rho_{lt}} [\rho_{ht}S_{lt} - \rho_{lt}S_{ht} + \rho_{\text{exp}}(H, T)(S_{ht} - S_{lt})]. \quad (7)$$

The results are shown as solid lines in Fig. 2*b*; the agreement is excellent, with no adjustable parameters. Measurements using single-crystal samples are underway to explore the effect of $\kappa(H, T)$ on the analysis.

The precise shape of the $c(H, T)$ curves depends on the form of the effective medium model chosen, being sharper the lower the percolation threshold. Nonetheless, it is clear that the metallic fraction increases rapidly below the transition temperature, but does not broaden in applied field to the same extent as the magnetization. It is useful, therefore, to explore under what circumstances this can occur. The essential feature of the Millis *et al.* model is that the effective Jahn-Teller coupling constant λ_{eff} is very near its critical value in the paramagnetic phase. There are two phase transitions to consider a zero-temperature polaronic transition at a critical coupling constant λ_c that would occur in the absence of Hund's rule coupling, and a double-exchange ferromagnetic transition at T_C for $\lambda_{eff} = 0$. The dependence of the bandwidth on magnetic order in the double exchange picture causes both λ_{eff} and T_C to depend on the temperature through the magnetization. We propose here a simplified mean-field model that reproduces the essential features of the microscopic calculation to demonstrate that $c(H, T)$ is a secondary order parameter, driven by the primary order parameter, namely the magnetization, and that it resembles the experimentally determined curves. We assume that the ferromagnetic free-energy functional is of conventional form

$$F_{mag} = \frac{1}{2}(T/T_C - 1)m^2 + \frac{1}{4}bm^4 - mh, \quad (8)$$

written in units of [20] $3Sk_B T_C/(S + 1) = 1.94k_B T_C$ for $S = 2(1 - x) + 3x/2 = 1.83$ and $x = 1/3$. Further, we have $h = g\mu_B(S + 1)H/3k_B T_C = H/2360$ kOe. The secondary parameter $c(H, T)$ is assumed to be driven by the difference $\lambda_{eff} - \lambda_c$. We approximate the dependence of λ_{eff} on the magnetization by writing $\lambda_{eff} - \lambda_c \propto \alpha - \gamma m^2 + \dots$, where α is small and positive. The electronic free energy can then be written, in the same dimensionless units as Eq. (8), as

$$F_{el} = \frac{1}{2}(\alpha - \gamma m^2)c^2 + \frac{1}{4}\beta c^4. \quad (9)$$

Minimizing the total free energy $F = F_{mag} + F_{el}$, we obtain

$$\frac{\partial F}{\partial m} = (T/T_C - 1 - \gamma c^2)m + bm^3 - h = 0 \quad (10)$$

$$\frac{\partial F}{\partial c} = (\alpha - \gamma m^2)c + \beta c^3 = 0 \quad (11)$$

From Eq. (11) it is obvious that the concentration of metallic electrons is zero until the magnetization reaches the value $m = \sqrt{\alpha/\gamma}$, beyond which point c increases. In the limit $\alpha \rightarrow 0$, c is proportional to m , with the result that $b \rightarrow b - \gamma^2/\beta$, signalling a tendency for the system to approach a tricritical point and first order transitions as the coupling constant is increased. Note that the existence of a non-zero concentration \bar{c} can be considered to increase the critical point to $(1 + \gamma\bar{c}^2)T_C$, causing the magnetization to increase more rapidly than would be the case without coupling to the metallic electron concentration.

To proceed, we recognize that Eq.(10) is the expansion of a Brillouin function,

$$m = B_S \left(\frac{3ST_C}{(S+1)T} [(1 + \gamma c^2)m + h] \right), \quad (12)$$

while the equation for c can be assumed to be a small- c expansion of

$$c = \tanh [(1 - \alpha + \gamma m^2)c]. \quad (13)$$

In Fig. 3 we show the simultaneous solutions of Eqs. (12 & 13) for $\alpha = 0.02$ and $\gamma = 0.3$ at $H = 0, 24$ kOe, and 48 kOe. Application of the magnetic field increases the temperature at which c becomes non-zero by 7% or 20 K, consistent with the experimental data in Fig. 3 and, unlike the magnetization, does produce a high-temperature tail in c . As no thermal factors are included in the definition of c , the concentration of free carriers does not approach unity, and therefore differs slightly from the experimental $c(H, T)$ obtained from Eq. (3). The abrupt appearance of band electrons in this model produces a kink in the zero field magnetization curve at the onset temperature, seen as a deviation from the $H = 0, \gamma = 0$ curve. The inset to Fig. 4 shows the inverse of magnetization data in an applied field of 1 kG taken on a single crystal of $\text{La}_{0.7}\text{Ca}_{0.3}\text{MnO}_3$, [21] along with H/m for the 24 kG data of Fig. 3. The experimental kink moves to higher temperature as the field is increased, as predicted by the model, but occurs further from the actual transition than the model predicts. The transition temperature for this sample, obtained by a scaling analysis of the data below the kink temperature, is 216 K. Clearly, the mean-field model proposed here cannot capture the precursive behavior due to critical fluctuations, important in the actual experiment, that would move the kink to higher temperatures.

As noted above, a number of other experimental probes have suggested the coexistence of localized and delocalized d-holes in the ferromagnetic state. Booth et al. [11] have defined the density of delocalized holes n_{dh} analogously to our Eq. (3) from the width of the Mn-O EXAFS peak. They suggest that $n_{dh} \propto \exp(3.5m)$, which leaves a finite density of delocalized carriers above T_C and a nearly linear increase in n_{dh} below. The fits for the mean-square width of the Mn-O bond length distribution, however, look remarkably like the magnetization itself. Louca, et al. [9], in a Sr-doped sample with comparable T_C , report a gradual change in the number of nearest Mn-O neighbors as the temperature is reduced below the critical point. They interpret their data in terms of a gradual transition from single-site to triple-site polarons, rather than to free carriers as favored here. Similar neutron data by Billinge, et al. [12] show that the O-O bond-length distribution begins to narrow below T_C in a manner similar to our $c(0, T)$. Recent Raman results [10] find two contributions in the Raman intensity a diffusive component associated with small polarons and a continuum contribution from free carriers. The relative intensities of these components have temperature dependences that are very similar to $1 - c(0, T)$ and $c(0, T)$, respectively.

That the field and temperature dependence of the thermopower can be deduced directly from resistivities and field-independent component Seebeck coefficients lends strong support to a picture in which conducting regions arise and percolate in the vicinity of the phase transition. The rapid decrease in resistance requires a low percolation threshold which in turn, points to stick-like, or stripe-like domains. [22] Our simple mean-field model ignores a number of features that should be included in a complete treatment. In particular, we have excluded a term m^2c because it leads to a first-order transition for all values of the parameters; we cannot rule it out on symmetry grounds. Similarly, there should be a mixing entropy in the electronic free energy which, at sufficiently high temperatures, will lead to thermal dissociation of the polarons. Finally, we have not included gradient terms and therefore ignore inhomogeneous thermal fluctuations that are certain to be significant in a system such as this where there are competing order parameters. Nonetheless, our phenomenological approach provides a qualitative understanding of the field and temperature dependence of the transport properties while correctly predicting the existence of kinks in the magnetization curves.

This work was supported in part by DOE Grant No. DEFG0291ER45439 through the Illinois Materials Research Laboratory. MJ acknowledges support from U.S. Department of Energy at Los Alamos National Laboratory, NM.

REFERENCES

- [1] A. J. Millis, P.B. Littlewood, and B. I. Shraiman, Phys. Rev.Lett.**74**, 5144 (1995).
- [2] H. Röder, J. Zang, and A. R. Bishop, Phys. Rev. Lett. **76**, 1356 (1996).
- [3] J. Tanaka *et al.*, Jou. Phys. Soc. Japan **51** 1236 (1982), H.Y. Hwang *et al.*, Phys. Rev. Lett. **75**, 914 (1995), M.F. Hundley *et al.*, Appl. Phys. Lett. **67**, 860 (1995), M.R. Ibarra *et al.*, Phys. Rev. Lett. **75**, 3541 (1995), J.J. Neumeier *et al.*, Phys. Rev. **B52**, R7006 (1995), J.-H. Park *et al.*, Phys. Rev. Lett. **76**, 4215 (1996), P. Dai *et al.*, Phys. Rev. **B54**, R3694 (1996), D.N. Argyriou *et al.*, Phys. Rev. Lett. **76**, 3826 (1996), G. Zhao *et al.*, Nature **381**, 676 (1996). R.H. Heffner *et al.*, Phys. Rev. Lett. **77**, 1869 (1996), etc.
- [4] M. Jaime, H.T. Hardner, M.B. Salamon, M. Rubinstein, P. Dorsey, and D. Emin, Phys. Rev. Lett. **78** 951 (1997). Also M. Jaime *et al.*, J. Appl. Phys. **81**, (1997).
- [5] C. Zener, Phys. Rev. **82**, 403 (1951); P. W. Anderson and H. Hasegawa, Phys. Rev. **100**, 675 (1955).
- [6] K. Kubo and N. Ohata, J. Phys. Soc. Jpn., **33**, 21 (1972).
- [7] A. J. Millis, R. Mueller, and B. I. Shraiman, Phys. Rev. **54**, 5389 (1996), *ibid.* **54**, 5405 (1996).
- [8] D. Emin and T. Holstein, Phys. Rev. Lett. **36**, 1492 (1976).
- [9] D. Louca, T. Egami, E.L. Brosha, H. Röder, and A.R. Bishop, Phys. Rev. B **56**, R8475 (1997).
- [10] S. Yoon, H.L. Liu, G. Schollerer, S.L. Cooper, P.D. Han, D.A. Payne, S.-W. Cheong, and Z. Fisk, Phys. Rev. B **58**, 2795 (1998).
- [11] C. H. Booth, F. Bridges, G.H. Kwei, J.M. Lawrence, A.L. Cornelius, and J.J. Neumeier, Phys. Rev. Lett. **80**, 853 (1998). Similar results are discussed by A. Lanzara *et al.*, Phys. Rev. Lett. (to be published).
- [12] S. J. L. Billinge, R.G. DiFrancesco, G.H. Kwei, J.J. Neumeier, and J.D. Thompson, Phys. Rev. Lett. **77**, 715 (1996).
- [13] R. Landauer in *Electrical Transport and Optical Properties of Inhomogeneous Media*, edited by J. C. Garland and D. B. Tanner (American Institute of Physics, New York, 1978) pg. 2.
- [14] M. Jaime, M. B. Salamon, K. Pettit, M. Rubinstein, R.E. Trece, J.S. Horwitz, and D.B. Chrisey, J. Appl. Phys. **68**, 1576 (1996).
- [15] M. Jaime, M.B. Salamon, M. Rubinstein, R.E. Trece, J.S. Horwitz, and D.B. Chrisey, Phys. Rev. B **54**, 11 914 (1996)
- [16] A. N. Lagarkov and A. K. Sarychev, Phys. Rev. B **52**, 6318 (1996).
- [17] J. P. Straley, J. Phys. D **14**, 2101 (1981).
- [18] D. Bergman and D. Stroud, in *Solid State Physics, vol. 46*, edited by H. Ehrenreich and D. Turnbull (Academic Press, New York, 1992) pg. 147.
- [19] D. W. Visser, A. P. Ramirez, and M. A. Subramanian, Phys. Rev. Lett. **78**, 3947 (1997); J.L. Cohn, J.J. Neumeier, C.P. Popoviciu, K.J. McClellan, and T. Leventouri, Phys. Rev. B **56**, R8495 (1997).
- [20] D. C. Mattis, *The Theory of Magnetism II*, (Springer-Verlag, Berlin, 1985) pg. 22.
- [21] S. H. Chun, et al. (to be published).
- [22] S-W. Cheong and C. H. Chen, in *Colossal Magnetoresistance and Related Properties*, edited by B. Raveau and C. N. R. Rao (World Scientific, in press).

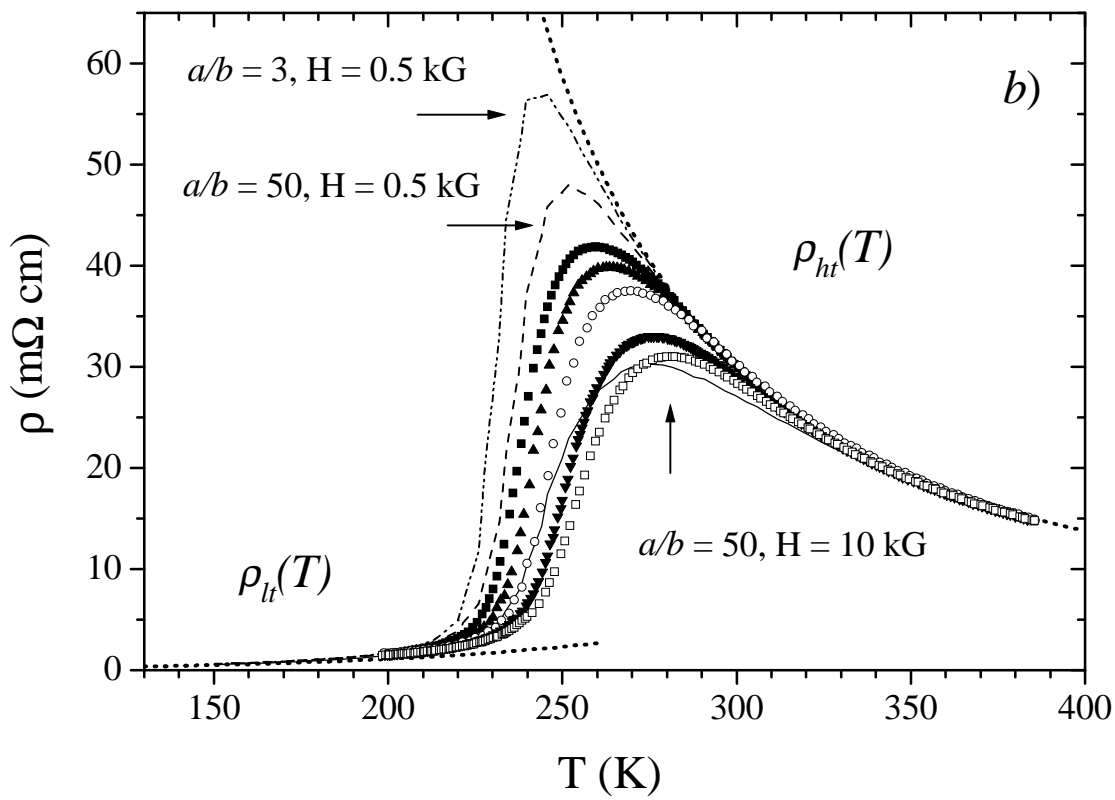
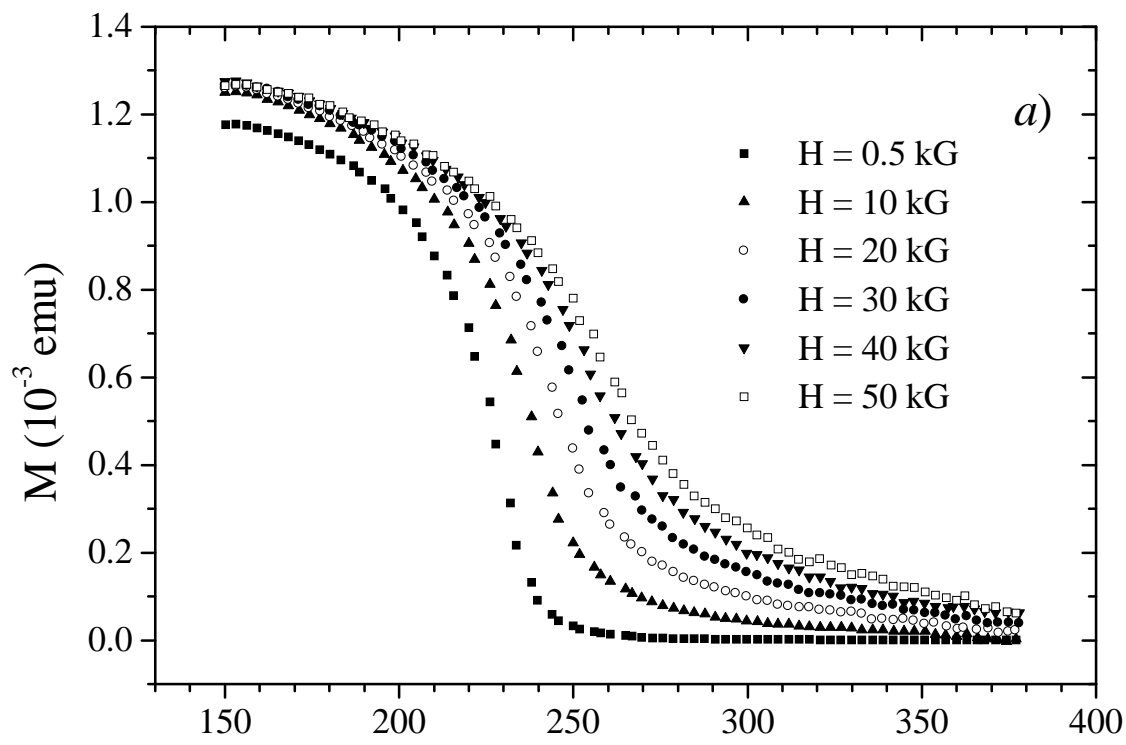
FIGURES

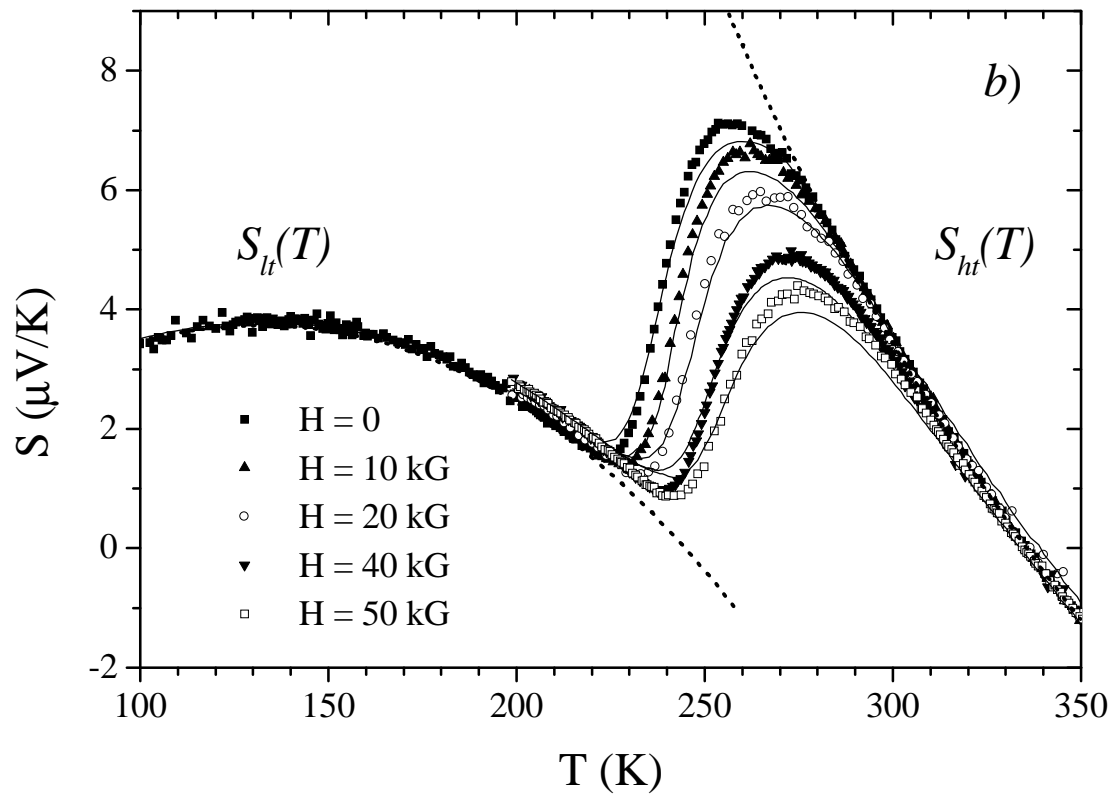
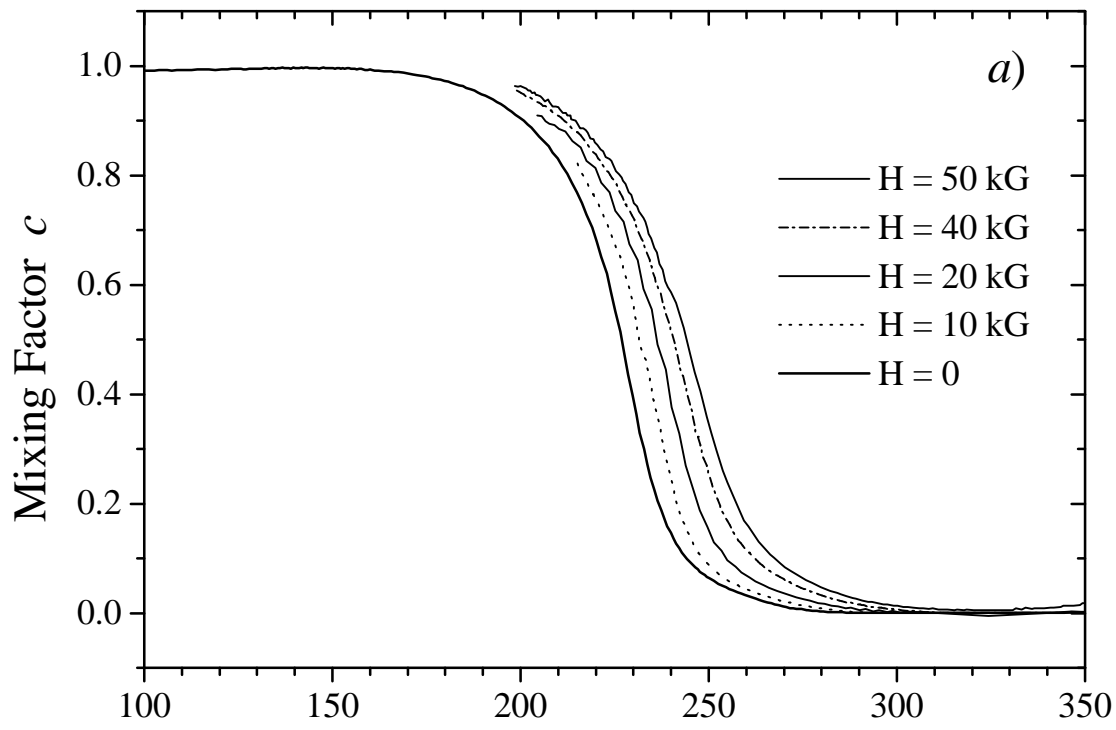
FIG. 1. (a) Magnetization data for this sample. (b) Resisitivity data as functions of field and temperature. The broken curves are effective field calculations at two values of a/b , assuming that the low field magnetization represents the metallic concentration. The solid line uses the magnetization measured at 10 kOe, and $a/b = 50$. Dotted lines are the low and high temperature limits discussed in the text.

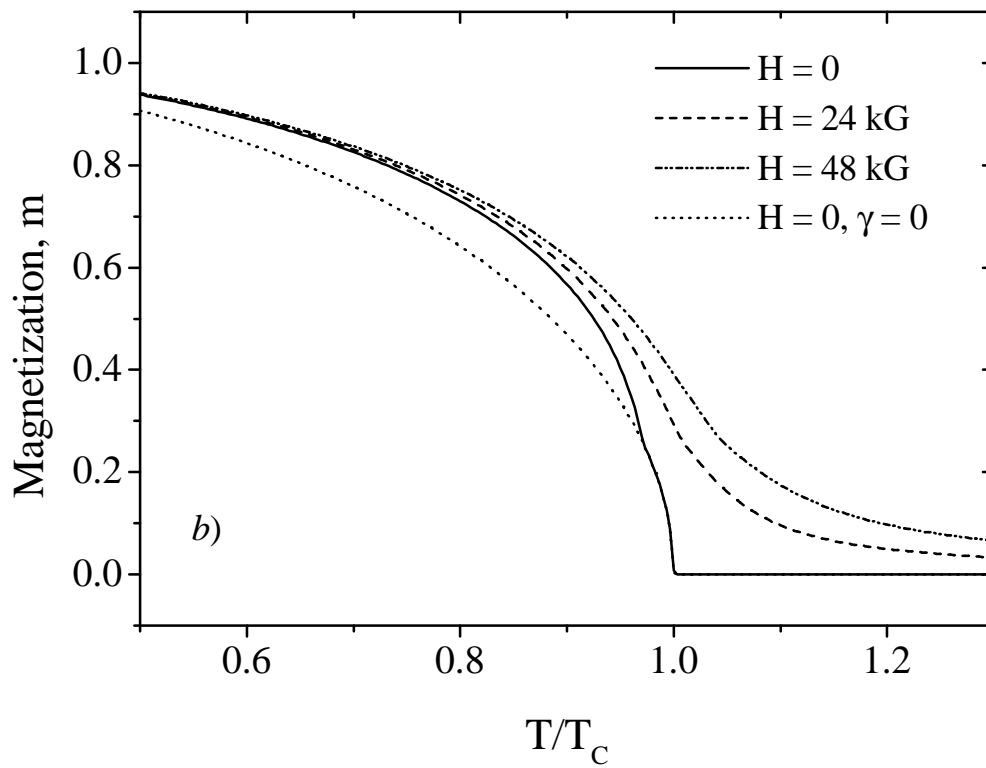
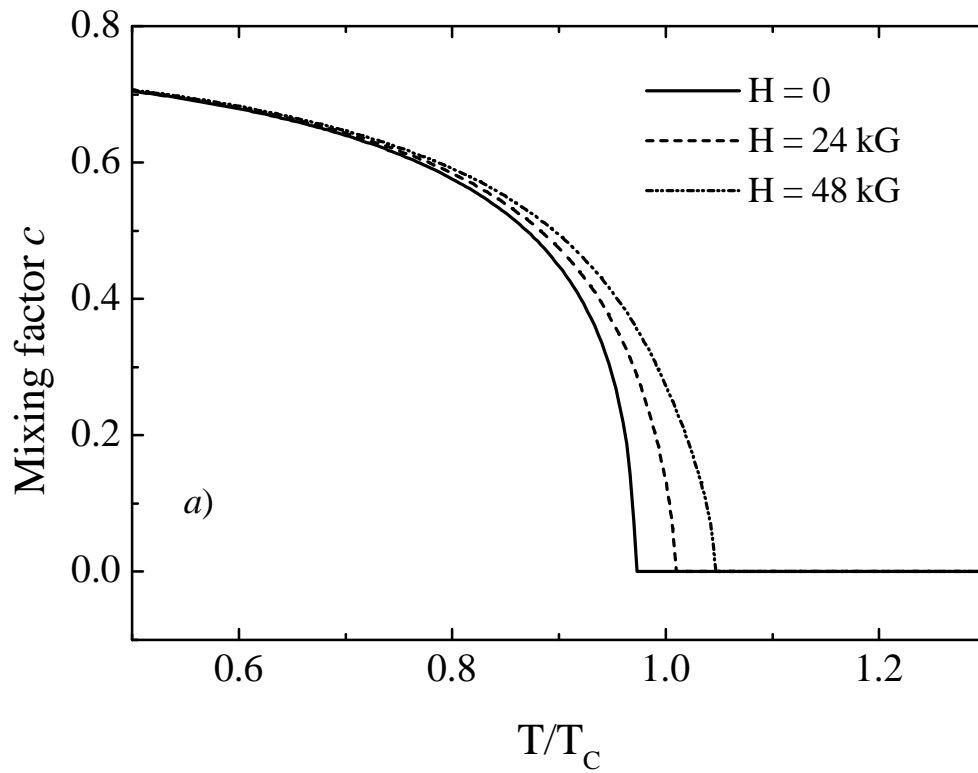
FIG. 2. (a) The mixing factor $c(H, T)$ extracted from the resisitivity using the effective medium approximation with $a/b = 50$. (b) Seebeck coefficient data and results of a computation using the measured resistivity $\rho_{exp}(H, T)$ as described in the text. Dotted lines show the low and high temperature fits.

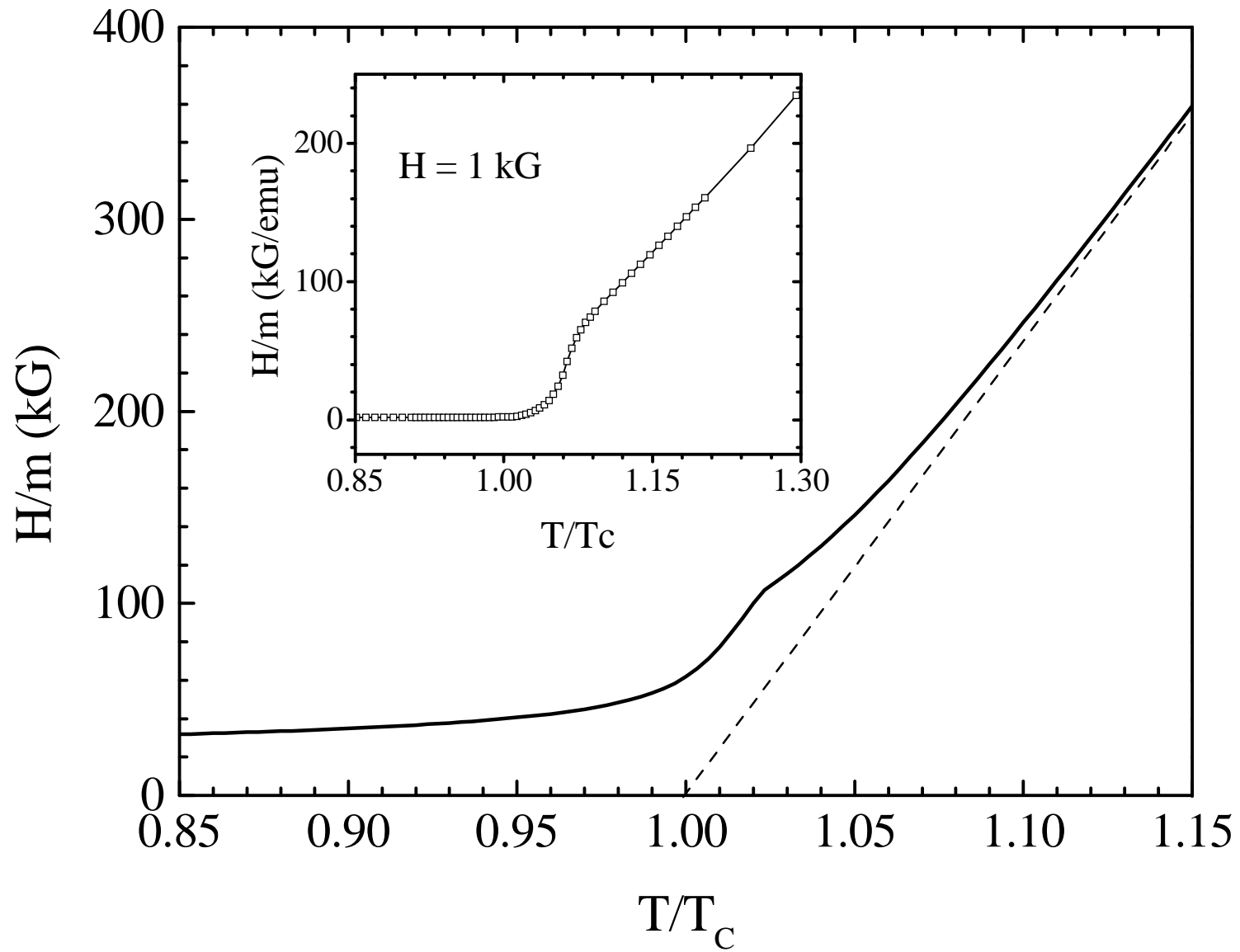
FIG. 3. (a) The mixing factor $c(H, T)$ calculated in the mean-field model with $\alpha = 0.02$ and $\gamma = 0.3$. (b) The magnetization calculated with the same parameters. The dotted line shows the non-interactive case for comparison.

FIG. 4. Inverse magnetic susceptibility H/m vs temperature near the M-I transition for $H = 24$ kOe. The dashed line is the zero field extrapolated behavior. The appearance of free carriers induce the rise of the effective T_C , leading to a kink in the susceptibility. Inset Inverse susceptibility of a single crystal sample of $\text{La}_{0.7}\text{Ca}_{0.3}\text{MnO}_3$, measured in a field of 1 kG.









"Coexistence of Localized...", M. Jaime *et al.* Figure 4